

Equipping Sketch Patches with Context-Aware Positional Encoding for Graphic Sketch Representation

Sicong Zang^{a,*}, Zhijun Fang^a

^a*School of Computer Science and Technology, Donghua University, Shanghai, 201620, China*

Abstract

The drawing order of a sketch records how it is created stroke-by-stroke by a human being. For graphic sketch representation learning, recent studies have injected sketch drawing orders into graph edge construction by linking each patch to another in accordance to a temporal-based nearest neighboring strategy. However, such constructed graph edges may be unreliable, since a sketch could have variants of drawings. In this paper, we propose a variant-drawing-protected method by equipping sketch patches with context-aware positional encoding (PE) to make better use of drawing orders for learning graphic sketch representation. Instead of injecting sketch drawings into graph edges, we embed these sequential information into graph nodes only. More specifically, each patch embedding is equipped with a sinusoidal absolute PE to highlight the sequential position in the drawing order. And its neighboring patches, ranked by the values of self-attention scores between patch embeddings, are equipped with learnable relative PEs to restore the contextual positions within a neighborhood. During message aggregation via graph convolutional networks, a node receives both semantic contents from patch embeddings and contextual patterns from PEs by its neighbors, arriving at drawing-order-enhanced sketch representations. Experimental results indicate that our method significantly improves sketch healing and controllable sketch synthesis.

Keywords: Graphic sketch representation, positional encoding, graph convolutional network, controllable sketch synthesis, sketch healing

1. Introduction

Free-hand sketches carry vivid emotions and messages for communication through human history. The drawing order of a sketch records how it is drawn stroke-by-stroke by a human being. It provides models a unique view to review how sketch components are organized by a sequential positional structure, which cannot be stored on the canvas by sketch images seen in daily life.

Recent studies have utilized the sequential information from sketch drawing orders to cooperate with the visual patterns from sketch images for representation learning. One common approach is employing a two-branch encoder to capture a pair of latent codes from a sketch image and its corresponding sketch sequence simultaneously, and further combine them for the final sketch representation [3, 4, 5, 6]. Another way is injecting drawing orders into graphic sketch representation by linking sketch patches according to drawing-order-based temporal proximity [1, 2]. The hybrid of temporal and visual features via sketch graphs is flexible and beneficial for learning accurate sketch representation.

Due to variations of sketch drawings, it is doubtful whether the sequential information stored in drawing orders could reveal

reliable relationships between sketch components, e.g., constructing graph edges as in [1, 2]. For example, as shown in Fig. 1, when drawing a pig face, its nose and ears could be drawn next to each other in order A, but are separated in B, which arrives at two different groups of graph edges with various sequential relationships among sketch components, shown in Fig. 1(a). If graph edges are constructed by such variable relationships, the passing messages over them for message aggregation via graph convolutional network (GCN) layers [7] might dilute or interrupt the target node. As a result, though no additional information from drawing order attends the representation learning, SP-gra2seq [8], which constructs graph edges in a more reliable way by semantic similarity, still outperforms Sketch-Healer [1] and SketchHealer 2.0 [2] on sketch representation learning.

It motivates us to make better use of sketch drawing orders by injecting them into graph nodes, shown in Fig. 1(b). More specifically, each sketch patch regarded as graph nodes are enriched by its sequential position encoded by a vectorized positional encoding (PE) [9, 10]. PEs record when a patch is drawn in a drawing order¹. We borrow the term *context* from the field of linguistics to describe the neighboring patches which surround a focal patch in a drawing order. By the attendance of PEs, the position-unaware graph nodes are equipped with con-

*Corresponding author

Email addresses: sczang@dhu.edu.cn (Sicong Zang), zjfang@dhu.edu.cn (Zhijun Fang)

¹The cropping centers of sketch patches are selected following the drawing orders [1, 2, 8]. Thus, we transplant the sequential positions in drawing order to rank patches.

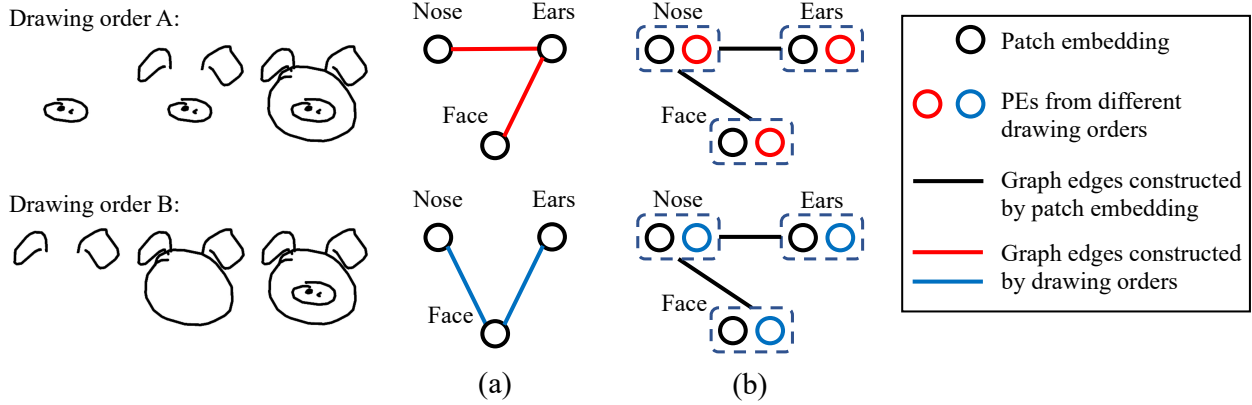


Figure 1: Two approaches to inject drawing orders into graphic sketch representation, when dealing with variants of sketch drawings. (a) Constructing graph edges by drawing orders as in [1, 2], i.e., linking the neighboring sketch components by a drawing order. (b) The proposed approach. We inject drawing orders into PEs, which only enrich graph nodes but never attend the edge construction.

textual information. During the message aggregation via GCN layers, each node receives not only the content of neighboring nodes but also when they are drawn in the timeline, guiding our method to capture more hidden patterns from the unique view of drawing. Moreover, our graph edges are constructed by semantic similarity between patches as in [8], leaving sequential positions away from node linking to protect graph construction from variants of sketch drawings.

To realize the above proposals, we propose Drawing-order-enhanced Context-aware graph to sequence (DC-gra2seq) to equip graphic sketch representation with drawing orders. Each patch embedding, captured by a convolutional neural network (CNN) encoder, is equipped with a sinusoidal absolute PE to highlight the sequential position in drawing orders. Moreover, its neighboring patches, which are ranked by the values of self-attention scores between patch embeddings, are offered with learnable relative PEs to restore the contextual positions within a neighborhood. Both patch embeddings and PEs are incorporated by a GCN encoder to obtain the final sketch representation, which is sent into a recurrent neural network (RNN) decoder for sketch generation. To summarize, we make the following contributions:

1. We propose DC-gra2seq to learn graphic sketch representation by introducing context-aware PE to make better use of sketch drawing orders.
2. We rethink the attendance of drawing orders in graphic sketch representation, and equip them on graph nodes to access the sequential positions from drawing orders, but keep them away from graph edges to protect sketch learning from variants of sketch drawings.
3. Experimental results indicate that DC-gra2seq achieves significant improvements on sketch healing and controllable sketch synthesis.

2. Related work

2.1. Learning sketch representations

Sketches are usually formed by raster images to restore visual patterns from the canvas, or formed by sequences of coordinates to record how they are drawn stroke-by-stroke by human. For sketch images, CNN-based methods, e.g., [11, 12, 13, 14], could be utilized for representation learning to capture the spatial dependencies among drawing strokes. For sketch sequences, in order to extract temporal relationships between strokes, RNN-based, e.g., [15, 16], or transformer-based methods, e.g., [17, 18] have been proposed to learn the contextual information along sketch drawing orders. Moreover, using dual-branch encoders, e.g., [3, 4, 6, 5], is beneficial to learn accurate and efficient latent representations from paired sketches (a sketch image and its corresponding sketch sequence), by making better use of both temporal and spatial relationships among sketch components.

Recently, graphic sketch representation is demonstrated as effective ways for sketch representation learning in sketch synthesis [1, 2, 19, 8], sketch recognition [20, 21, 22], sketch segmentation [23, 24] and sketch-based image retrieval [25]. A sketch is formed as a graph with multiple components, whose captured features are aggregated by graph neural network (GNN) [26] or GCN layers to obtain the final sketch representation. Graph nodes can be sketch patches cropped from sketch images [1, 2, 8], coordinates on the latticed canvas [19], etc, which carry local sketch patterns. Graph edges can be constructed by linking sketch components to follow sketch drawing order [1, 2], Euclidean distances between sketch components [19, 24], or semantic similarity [8], etc. Graphic representation enables the message passing between sketch components for learning better sketch representation.

We aim to equip graph nodes with contextual positions from sketch drawing order via PEs, which makes message aggregating process via GCN layers context-aware for learning accurate sketch representations.

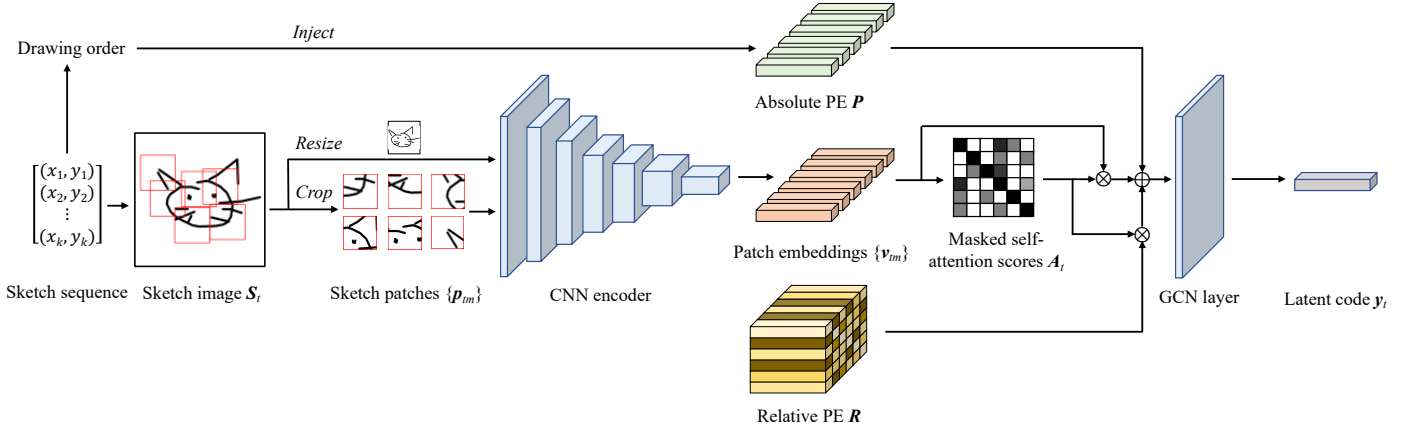


Figure 2: Learning graphic representation y_t of sketch S_t by DC-gra2seq. The cropped sketch patches $\{p_m\}$ along with the resized full sketch p_0 are embedded by a CNN encoder as patch embeddings $\{v_m\}$. The absolute PE P embedded by original sketch drawing order and the relative PE R restoring contextual positions between patches are incorporated with $\{v_m\}$, weighted by the masked self-attention scores A_t computed by solo $\{v_m\}$. A GCN layer collects the aggregated messages to produce the final sketch code y_t .

2.2. Positional encoding

Positional encoding makes better use of some valuable sequential or structural information, when training position-unaware networks, e.g., self-attention network [10] and graph attention network (GAT) [27]. PEs give these architectures a sense of which portion of the sequence in input (or output) it is currently dealing with. Recent studies embedded the positional information by absolute [9, 10], relative PEs [28, 29, 30] or both [31]. Absolute PEs restore the absolute positions of the input tokens, indicating where a specific token is located in a sequence or a canvas. Relative PEs encode the relative pairwise distances or positions of a pair of tokens, which is invariant to the position of focal token in contrast to absolute PE. The positional information can be embedded by either fixed [10, 31] or learnable PEs [9, 28, 30, 32, 33].

We inject sketch drawing orders into graph nodes in graphic sketch representation by equipping sketch patches with both absolute and relative PEs. Each patch collects the information from its neighboring patches along with their corresponding PEs during a message aggregating process.

3. Methodology

Fig. 2 offers an overview to indicate how DC-gra2seq learns graphic sketch representation. The embeddings of the cropped sketch patches as graph nodes are captured by a CNN encoder, and the graph edges between them are constructed by the masked self-attention scores computed from solo patch embeddings. During message aggregation via a GCN layer, both absolute and relative PEs are equipped on graph node to make use of the sequential and contextual positions in drawing orders. And the final sketch code is fed into an RNN decoder to reconstruct the input sketch in a sequence form.

3.1. Injecting sketch drawing order into PE

For the t -th sketch image $S_t \in \mathbb{R}^{640 \times 640}$ as input, we crop M sketch patches $\{p_m\}_{m=1}^M$ with the size of 256×256 from the

canvas. We adopt the selecting rule utilized in [1, 2, 8] to determine the cropping centers of patches, which arranges these patches in a sequential order in accordance to the drawing orders. More specifically, as the cropping center of p_m is located on the stroke drawn before the one of $p_{t,m+1}$, p_m is positioned prior to $p_{t,m+1}$ in the sequential order. Such sequential information makes patches position-aware, and we name the patches surrounding a focal one in the drawing order **contexts** of one another.

In order to make use of the sequential information, we firstly inject sketch drawing orders into sinusoidal **absolute PE** [10], shown in Eq. (1).

$$\begin{aligned} P(pos, 2d) &= \sin(pos/10000^{2d/512}), \\ P(pos, 2d+1) &= \cos(pos/10000^{2d/512}), \end{aligned} \quad (1)$$

where pos and d denote the position and dimension, respectively. 512 indicates the length of vectorized PE. $P(m, \cdot)$ (abbreviated as $P(m)$ in the following) indicates the absolute PE of p_m to record when p_m is drawn in a drawing order. Absolute PEs enrich the position-unaware sketch patches with sequential hints, which cannot be captured from canvas, and their attendances in sketch learning guide DC-gra2seq to consider both visual patterns and sequential information jointly.

Secondly, in order to encode the contextual distances between sketch patches along the drawing order, we introduce the **learnable relative PE**, $R(i, j)$ to represent the contextual distance between patches p_{ti} and p_{tj} . Each $R(i, j)$ is a learnable vector with the same length of $P(i)$, and we restrict $R(i, j)$ with the following three conditions:

$$R(i, i+k) = R(j, j+k), \quad (2)$$

$$R(i, j) = R(j, i), \quad (3)$$

$$R(i, i) = \mathbf{0}. \quad (4)$$

Our relative PE is *target-invariant* in Eq. (2), i.e., a relative PE is only sensitive to the contextual distance between

patches, but is invariant with the contents of patches. Two pairs of patches with the same contextual distance, e.g., $(\mathbf{p}_{ti}, \mathbf{p}_{t,i+k})$ and $(\mathbf{p}_{tj}, \mathbf{p}_{t,j+k})$ share the same value of relative PE. Our relative PE is *undirected* in Eq. (3), i.e., it does not have orientations. Finally, we also fix the relative PE between one patch and itself at the token $\mathbf{0}$ with all elements valued by zero.

As a result, for a sketch represented by M sketch patches, totally M vectorized relative PEs are required in DC-gra2seq.

3.2. Context-aware graphic sketch representation

For the M sketch patches cropped from the full sketch \mathbf{S}_t , a CNN encoder $q_\phi(\mathbf{v}|\mathbf{p})$, which contains seven convolutional layers (channel numbers as 8, 32, 64, 128, 256, 512 and 512) with 2×2 kernels and the ReLU activation function followed by max pooling and batch normalization, is employed to capture the patch embeddings $\mathbf{v}_{tm} \in \mathbb{R}^{512 \times 1}$ of \mathbf{p}_{tm} . \mathbf{v}_{tm} , regarded as a graph node, shares the same length with \mathbf{P} and \mathbf{R} .

We link the sketch patches \mathbf{p}_{ti} and \mathbf{p}_{tj} to construct a graph edge by considering their self-attention score $\alpha_t^{\text{atten}}(i, j)$, computed by their patch embeddings \mathbf{v}_{ti} and \mathbf{v}_{tj} . In practice, we implement the attention operation by using the cosine similarity, which is named as synonymous proximity in [8].

$$\alpha_t^{\text{atten}}(i, j) = \frac{\mathbf{v}_{ti}^\top \mathbf{v}_{tj}}{\|\mathbf{v}_{ti}\|_2 \cdot \|\mathbf{v}_{tj}\|_2}, \quad (5)$$

where $\|\cdot\|_2$ denotes the L2 norm. A large value of $\alpha_t^{\text{atten}}(i, j)$ indicates that the patch \mathbf{p}_{ti} is highly relevant to \mathbf{p}_{tj} in content. It is worth noting that neither the absolute PE nor relative PE attends the calculation of attention scores. The absence of PEs reduces the uncertainty brought by variants of sketch drawings, driving to reliable edge constructions for the passing message aggregation.

We utilize the computed self-attention score $\alpha_t^{\text{atten}}(i, j)$ in Eq. (5) to construct graph edges, and each node is only linked to the ones with the top-2 largest values among $\{\mathbf{v}_{tm}\}_{m \neq i}$. We arrive at the masked attention scores, stored in an adjacency matrix \mathbf{A}_t , with the element $\mathbf{A}_t(i, j)$ in i -th row and j -th column computed by,

$$\mathbf{A}_t(i, j) = \begin{cases} 1, & j = i, \\ 0.5 \cdot \alpha_t^{\text{atten}}(i, j), & j = j^*, \\ & j^* = \arg \max_{m \neq i} \alpha_t^{\text{atten}}(i, m), \\ 0.2 \cdot \alpha_t^{\text{atten}}(i, j), & j = j', \\ & j' = \arg \max_{m \neq i, j^*} \alpha_t^{\text{atten}}(i, m), \\ 0, & \text{otherwise.} \end{cases} \quad (6)$$

Following the settings in [8], we offer the top-2 neighbors with the weights 0.5 and 0.2, according to their importance to allow the more relevant neighbor to transport more beneficial messages towards the target node during the aggregation process by the following GCN encoder.

Eq. (7) presents the message aggregating process for node \mathbf{v}_{ti} via a single GCN layer.

$$\mathbf{v}_{ti}^{\text{aggr}} = \sum_{\mathbf{v}_{tj} \in \{\mathcal{N}(\mathbf{v}_{ti}), \mathbf{v}_{ti}\}} \left[\mathbf{A}_t(i, j)(\mathbf{v}_{tj} + \mathbf{R}(i, j)) \right] + \mathbf{P}(i), \quad (7)$$

where $\mathcal{N}(\mathbf{v}_{ti})$ denotes the neighborhood of \mathbf{v}_{ti} determined by the masked self-attention scores in Eq. (6).

The target node \mathbf{v}_{ti} receives the passing messages containing both the patch embedding \mathbf{v}_{tj} and its corresponding relative PE $\mathbf{R}(i, j)$, from the neighbors. A neighboring node not only delivers its semantic content captured from sketch patch but also the contextual position between them. After incorporating all the passing message weighted by their attention score $\mathbf{A}_t(i, j)$, DC-gra2seq is able to learn what the neighboring nodes contain to benefit the target \mathbf{v}_{ti} and to check how far their contextual distances are toward \mathbf{v}_{ti} . Moreover, we further incorporate \mathbf{v}_{ti} with its absolute PE $\mathbf{P}(i)$ to highlight where \mathbf{v}_{ti} is positioned in the drawing order. Especially, both absolute and relative PEs only participate in node aggregation to enrich the patch embedding with sequential and contextual positions, but are kept away from the edge construction in \mathbf{A}_t , driving to variant-drawing-protected sketch representation.

In practice, a GCN encoder $q_{\xi, \mathbf{R}}(\mathbf{y}|\mathbf{V}, \mathbf{A})$ is introduced to incorporate all patch embeddings along with their absolute and relative PEs. Furthermore, a full sketch embedding \mathbf{v}_{t0} , which is also captured by the CNN encoder q_ϕ from a 256×256 image \mathbf{p}_{t0} resized from the original full sketch \mathbf{S}_t , is also taken into account during message aggregation. Eq. (8) presents the GCN layer.

$$\boldsymbol{\mu}_t, \boldsymbol{\sigma}_t = \text{MLP} \left[\tilde{\mathbf{D}}_t^{-\frac{1}{2}} \tilde{\mathbf{A}}_t \tilde{\mathbf{D}}_t^{-\frac{1}{2}} (\tilde{\mathbf{V}}_t^\top + \tilde{\mathbf{R}}^\top) + \tilde{\mathbf{P}}^\top \right], \quad (8)$$

$$\tilde{\mathbf{V}}_t = [\mathbf{v}_{t0}, \mathbf{V}_t] = [\mathbf{v}_{t0}, \mathbf{v}_{t1}, \dots, \mathbf{v}_{tM}],$$

$$\tilde{\mathbf{A}}_t = \begin{bmatrix} 0.5 & \mathbf{0}^\top \\ 0.5 \cdot \mathbf{1} & \mathbf{A}_t \end{bmatrix}, \tilde{\mathbf{P}} = [\delta_0, \mathbf{P}], \tilde{\mathbf{R}} = [\delta'_0, \mathbf{R}], \quad (9)$$

where $\tilde{\mathbf{D}}_t$ is the degree matrix of $\tilde{\mathbf{A}}_t$. $\tilde{\mathbf{A}}_t$, $\tilde{\mathbf{V}}_t$, $\tilde{\mathbf{R}}$ and $\tilde{\mathbf{P}}$, which are defined in Eq. (9), contain static placeholders ($\mathbf{0}, \mathbf{1}, \delta_0, \delta'_0 \in \mathbb{R}^{M \times 1}$) to fit the matrix calculation with the newly introduced embedding \mathbf{v}_{t0} . These placeholders are vectors with fixed values which cannot be trained. We incorporate the features extracted in a global view from the full sketch with the ones captured from sketch patches with local sketch details for the final sketch representation.

MLP(\cdot) in Eq. (8) stands for a multi-layer perception, which produces the vectors $\boldsymbol{\mu}_t$ and $\boldsymbol{\sigma}_t$ to compute the final sketch representation $\mathbf{y}_t = \boldsymbol{\mu}_t + \boldsymbol{\sigma}_t \odot \boldsymbol{\epsilon}$ via reparameterization [34]. $\boldsymbol{\epsilon}$ is randomly sampled from the standard Gaussian distribution $\mathcal{G}(\boldsymbol{\epsilon}|\mathbf{0}, \mathbf{I})$.

3.3. Training a DC-gra2seq

We feed the captured sketch representation \mathbf{y}_t into an RNN decoder $p_\theta(\mathbf{S}|\mathbf{y})$, which is adopted from [15], to reconstruct the input sketch in a sequential format. Our objective is to maximize the log-likelihood term,

$$\mathcal{L}(\boldsymbol{\theta}, \boldsymbol{\phi}, \boldsymbol{\xi}, \mathbf{R}|\mathbf{S}) = \sum_{t=1}^N \mathbb{E}_{q_{\boldsymbol{\phi}, \boldsymbol{\xi}, \mathbf{R}}(\mathbf{y}_t|\mathbf{S}_t)} \log p_\theta(\mathbf{S}_t|\mathbf{y}_t). \quad (10)$$

Though DC-gra2seq falls into the variational auto-encoder (VAE) [34] framework, we follow [1, 2, 8, 11] to remove the Kullback-Leibler (KL) divergence term from the objective to learn sketch representation more freely.

Table 1: Controllable sketch synthesis performance (%). “@ k ” indicates the top- k accuracy.

Model	DS1				DS2				DS3			
	<i>Rec</i> ↑	<i>Ret</i> ↑			<i>Rec</i> ↑	<i>Ret</i> ↑			<i>Rec</i> ↑	<i>Ret</i> ↑		
		@1	@10	@50		@1	@10	@50		@1	@10	@50
sketch-pix2seq [11]	83.99	13.45	30.12	49.99	85.46	50.94	71.38	80.15	79.13	22.92	47.55	58.19
Song et al. [3]	91.77	16.41	36.43	52.22	86.98	58.84	76.84	80.06	83.28	25.47	43.39	56.16
Xu et al. [5]	93.32	22.70	54.40	75.04	90.01	51.98	75.79	83.26	82.34	25.25	54.04	72.90
RPCL-pix2seq [12]	93.18	17.86	38.87	55.30	88.73	53.19	71.60	87.91	81.80	28.80	59.05	77.52
RPCL-pix2seqH [13]	94.97	71.36	90.29	94.86	92.62	85.91	93.67	95.90	87.82	81.22	92.15	94.90
SketchHealer [1]	91.04	58.80	82.15	91.33	94.04	87.54	96.19	98.26	87.03	68.52	82.37	86.57
SketchHealer 2.0 [2]	93.13	57.19	84.54	90.26	90.94	87.37	94.59	97.60	87.37	50.67	76.11	82.42
SketchLattice [19]	75.91	6.55	14.01	26.72	71.80	6.91	14.76	28.82	62.21	5.90	10.36	19.39
SketchLattice ⁺	95.18	72.74	91.60	97.14	94.30	90.56	97.78	99.27	89.49	87.27	96.82	98.98
SP-gra2seq [8]	95.91	94.88	99.11	99.72	94.85	90.83	98.29	99.08	89.83	94.05	98.72	99.57
DC-gra2seq	96.26	96.84	99.48	99.88	95.70	92.75	98.08	99.42	90.41	96.27	99.47	99.81

4. Experiments and analysis

We testify our DC-gra2seq on two tasks, controllable sketch synthesis [12] and sketch healing [1], aiming to verify whether DC-gra2seq learns accurate and robust sketch representations.

4.1. Preparations

Datasets. Three datasets from QuickDraw [15] are selected, and all of them are adopted from [8] to make a direct comparison with the state-of-the-art SP-gra2seq [8]. Dataset 1 (DS1), which contains bee, bus, flower, giraffe and pig, evaluates representing performance on large variations of sketches within the same category. Dataset 2 (DS2), which collects airplane, angel, apple, butterfly, bus, cake, fish, spider, the Great Wall and umbrella, evaluates whether the models are sensitive to categorical patterns. Dataset 3 (DS3) collects the five categories in DS1 along with three new ones (car, cat and horse). Sketches in different categories are with shared stylistic patterns, e.g., both giraffes and horses can head left or right. Each category contains 70K training, 2.5K valid and 2.5K test sketches (1K = 1000).

Baselines. We compare DC-gra2seq with ten baseline models. Song et al. [3] and Xu et al. [5] learn representations from sketch images and their corresponding sketch sequences simultaneously. Sketch-pix2seq [11] learns representations from sketch images only. We make them a group to verify the advantage brought by drawing orders as an additional source. RPCL-pix2seq [12] and RPCL-pix2seqH [13] both constrain sketch codes with a specific distribution. SketchLattice [19], SP-gra2seq [8], SketchHealer [1] and SketchHealer 2.0 [2] learn graphic sketch representations. The sequential information from drawing orders are not used in SketchLattice and SP-gra2seq, while they are treated as prior knowledge to construct graph edges in SketchHealer and SketchHealer 2.0. Moreover, following [8], we provide SketchLattice⁺ to replace the original node embeddings captured from coordinates on lattice with the ones from sketch patches, to make a fair comparison.

Metrics. We use *Rec* and *Ret* [12] for evaluation. *Rec* describes whether a generated sketch \hat{S}_t and its corresponding input S_t are in the same category. We pre-train three sketch-a-net [35] classifiers to compute *Rec* for three datasets, respectively.

Ret indicates whether \hat{S}_t is successfully controlled by preserving both categorical and stylistic patterns from S_t . When calculating *Ret* for S_t , we obtain its code y_t and the reconstruction \hat{S}_t . We retrieve y_t from the gallery $Y = \{y_t(S_t) | S_t \in \text{test set}\}$ with the code \hat{y}_t of \hat{S}_t , and *Ret* indicates the successful retrieving rate. Both *Rec* and *Ret* are calculated from the entire test set.

When training a DC-gra2seq, the patch number M and the mini-batch size N are fixed at 20 and 256, respectively. We adopt the Adam optimizer to learn DC-gra2seq, and the learning rate starts from 10^{-3} with a decay rate of 0.95 after each training epoch.

4.2. Controllable sketch synthesis

Controllable sketch synthesis requires a model to generate sketches with the expected categorical and stylistic patterns. Table 1 reports the quantitative performances on three datasets.

Song et al. and Xu et al. outperform sketch-pix2seq as their sketch representations are enhanced by additional information from drawing orders. For graphic representation learning models, though SketchHealer and SketchHealer 2.0 are equipped with sketch drawing orders, they are defeated by SketchLattice⁺ and SP-gra2seq, which never utilize the sequential information as assistance. It is because the variations of sketch drawings drive to unreliable edge constructions, and the passing messages along these edges could dilute or interrupt the target patch learning.

The proposed DC-gra2seq injects drawing orders into context-aware PEs. The sequential positions of sketch patches are embedded on graph nodes, but never participate in valuing the relationships between patches, i.e., edge construction. As a result, the position-embedded PEs provide the captured patch embeddings with contextual information, which cannot be extracted from the canvas, guiding DC-gra2seq to realize when each patch is drawn along the drawing order. In the meantime, DC-gra2seq links patches by patch embeddings only, which stabilizing the message passing between patches with synonymous contents. Thus, DC-gra2seq achieves the best controllable synthesis performance, especially on top-1 (@1) *Ret*.

Table 2: Sketch healing performance (%). ‘‘Mask’’ denotes the probability for creating masks. ‘‘SH’’, ‘‘SL’’, ‘‘SP’’ and ‘‘DC’’ indicate SketchHealer, SketchLattice, SP-gra2seq and the proposed DC-gra2seq, respectively.

Mask	Model	DS1				DS2				DS3			
		<i>Rec</i> ↑	<i>Ret</i> ↑			<i>Rec</i> ↑	<i>Ret</i> ↑			<i>Rec</i> ↑	<i>Ret</i> ↑		
			@1	@10	@50		@1	@10	@50		@1	@10	@50
10%	SH [1]	70.38	14.25	27.91	45.51	70.56	35.22	55.86	66.24	60.91	15.10	37.89	53.10
	SH 2.0 [2]	90.18	19.45	41.51	59.94	87.07	39.40	64.01	81.20	76.45	15.55	39.99	61.67
	SL [19]	54.18	1.09	5.48	14.00	52.97	1.34	6.86	17.41	44.14	0.71	4.19	11.36
	SL ⁺	89.98	19.86	43.59	63.70	90.52	46.98	70.21	83.12	78.28	22.56	44.89	62.11
	SP [8]	92.90	41.24	65.74	80.16	91.24	50.42	73.35	85.18	83.38	40.20	63.40	77.52
	DC (ours)	94.45	74.59	88.83	94.31	92.64	67.61	84.31	91.17	85.21	71.66	86.34	92.35
30%	SH [1]	59.00	0.23	3.48	10.76	61.26	7.98	19.04	35.03	48.90	0.43	7.36	15.79
	SH 2.0 [2]	79.05	4.66	14.54	28.44	75.08	10.05	24.51	39.57	60.74	3.75	11.66	22.36
	SL [19]	32.03	0.08	2.05	5.96	31.73	0.88	3.64	9.25	23.06	0.41	2.41	5.96
	SL ⁺	70.91	1.02	5.26	14.28	81.76	10.43	26.44	42.90	67.31	2.75	11.13	23.68
	SP [8]	84.85	12.87	29.39	45.58	82.85	12.19	29.37	46.53	71.07	5.65	17.40	32.90
	DC (ours)	86.50	30.30	51.38	65.84	84.62	29.92	49.26	62.44	72.84	27.64	47.34	60.61

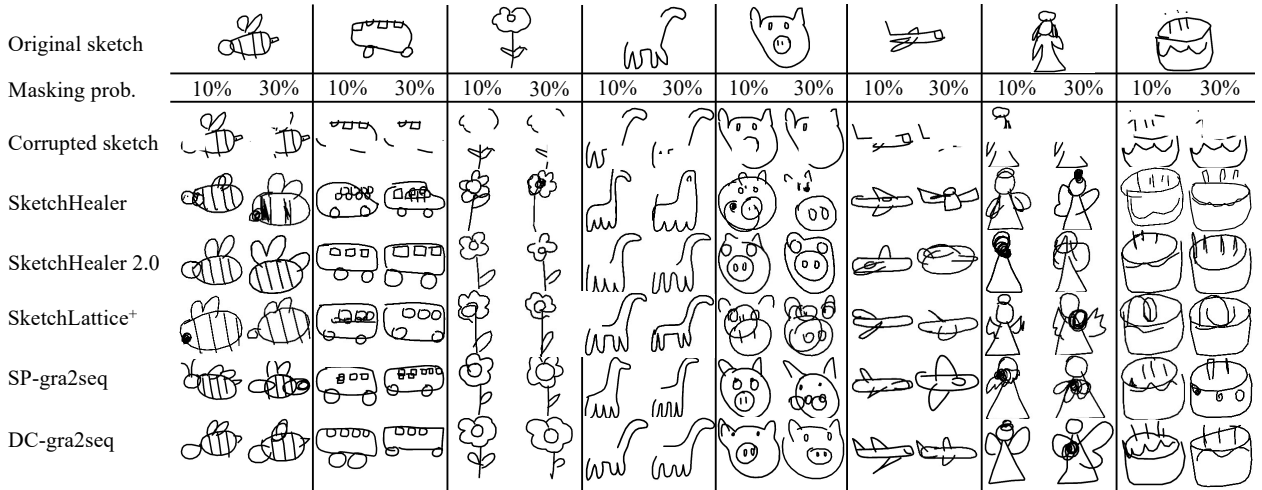


Figure 3: Qualitative comparisons on sketch healing.

4.3. Sketch healing

Sketch healing [1] requires a model to recreate a full sketch \hat{S}_t from the corrupted sketch S_t^m with masks. The generated \hat{S}_t is expected to preserve both categorical and detailed stylistic characteristics from the original unmasked S_t (S_t^m is corrupted from S_t). We adopt the approach utilized in [8] to mask sketches: After selecting the cropping centers for sketch patches, each center is applied with a masking probability of 10% or 30% for positioning a 256×256 mask on that location on the canvas. For SketchLattice and SketchLattice⁺, the coordinate selection on lattice is proceeded after applying masks.

We still evaluate sketch healing by *Rec* and *Ret* following [8], but adjust *Ret* to fit this task. Firstly, we mask S_t to get the corrupted sketch input S_t^m , which is sent into a model to generate \hat{S}_t . Then we compute the codes y_t and \hat{y}_t for S_t and \hat{S}_t , respectively. Finally, we retrieve the exact y_t from $Y = \{y_t(S_t) | S_t \in \text{test set}\}$ with \hat{y}_t to compute *Ret*. It is worth noting that each sketch is banded with the same masks during the metrics calculation for different models to make the com-

parison fair.

Table 2 presents the sketch healing results on three datasets. Our DC-gra2seq yields significant improvements on *Ret*. When dealing with sketch patches corrupted by masks, the passing messages from the semantic-related patches by self-attention scores could contain valuable missing information under the masks. Moreover, by taking account of PEs, DC-gra2seq might realize where these semantic-related patches are drawn from the contextual positions in a drawing order. By incorporating both visual patterns from the canvas and their sequential information from the embedded PEs, DC-gra2seq learns much more comprehensive and accurate sketch representations.

We also present some sketch healing results in Fig. 3, as qualitative comparisons. When facing a masking probability of 30%, some key characteristics of sketches are corrupted, e.g., a pig with missing nose. By making use of drawing orders, DC-gra2seq could access where these masked patches are drawn in the drawing order, and collect messages from contextual patches to generate a recognizable pig from the remaining

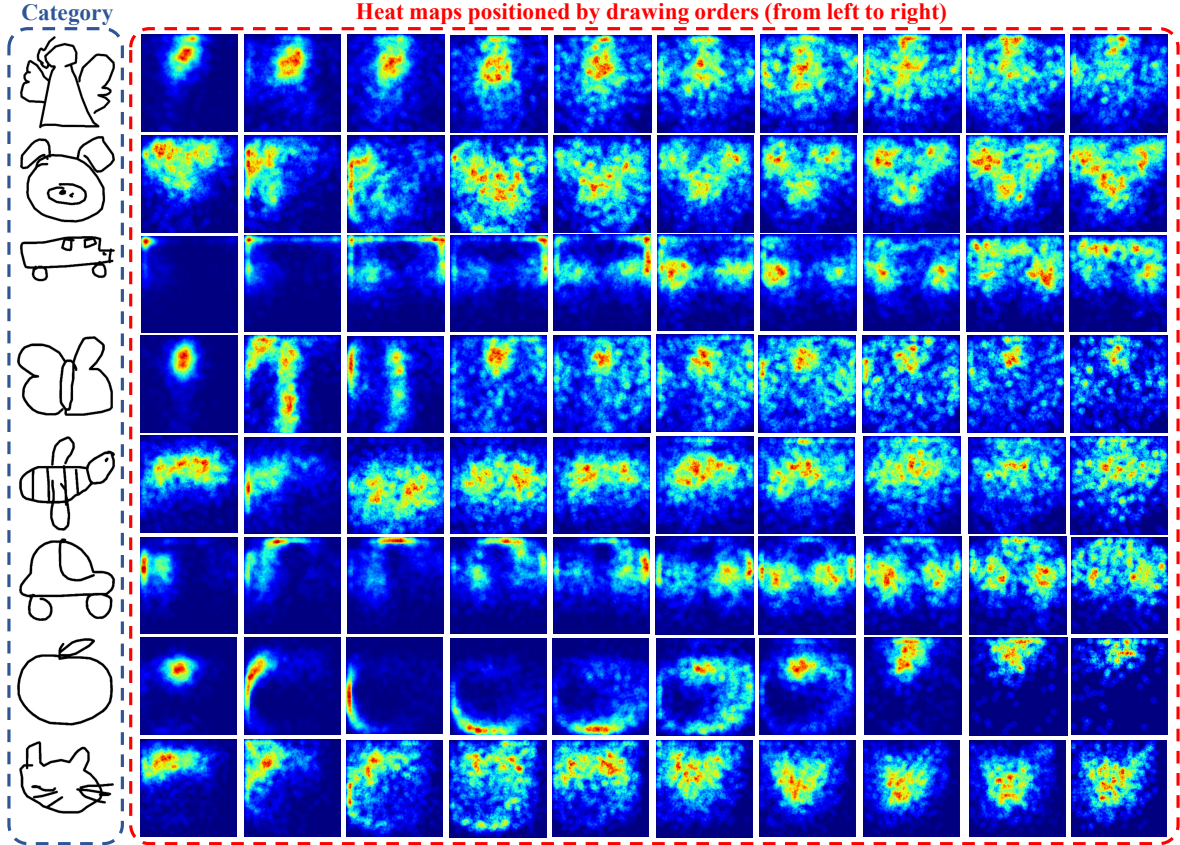


Figure 4: Variations of sketch drawings revealed by spatial heat maps on eight exemplary categories (angel, pig, bus, butterfly, bee, car, apple and cat), respectively. In each row, the heat maps from left to right are organized by sketch drawing orders. A heat map reports the magnitude where the next sketch component would be drawn on the canvas, and the red regions indicate the positions with a large probability to meet the next stroke at that moment.

Table 3: Controllable sketch synthesis performance (%) respectively computed on every single category in DS1. By checking each column, we figure out that pigs contribute the least to the performance on the full DS1, due to serious variants of sketch drawings revealed by Fig. 4.

Category	SketchHealer 2.0 [2]			SP-gra2seq [8]			DC-gra2seq					
	Rec	Ret		Rec	Ret		Rec	Ret				
		@1	@10	@50		@1	@10	@50		@1	@10	@50
Bee	89.52	30.72	57.60	75.72	93.48	92.16	96.36	98.92	94.20	97.44	99.64	99.96
Bus	98.60	57.44	83.88	94.24	98.88	97.00	99.38	99.89	99.00	97.12	99.64	100.00
Flower	94.52	33.16	62.08	79.56	96.76	91.28	94.16	97.32	98.36	96.80	99.12	99.72
Giraffe	94.48	41.96	75.20	91.96	96.16	87.52	98.94	99.76	96.84	97.48	99.88	100.00
Pig	89.20	24.76	51.76	73.20	92.88	83.56	90.68	96.32	93.72	96.64	99.76	99.96
Full DS1	93.13	57.19	84.54	90.26	95.91	94.88	99.11	99.72	96.26	96.84	99.48	99.88

face counter.

4.4. Variant-drawing-protected DC-gra2seq

This section aims to verify whether our DC-gra2seq could reduce the impact brought by variants of sketch drawings, to further achieve robust sketch representations.

We figure out that sketches in some category suffer more serious variants of sketch drawings than the others. Fig. 4 visualizes the degree of variants by using heat maps on eight exemplary categories. Each row contains ten heat maps positioned by sketch drawing order from left to right. And each map reports the magnitude where the next sketch component will be drawn on the canvas. The red regions indicate the positions

with a large probability to meet the next stroke at that moment. By reviewing the heat maps in a row from left to right, we can realize how serious the variants of drawings are for a category. For example, drawing a pig is more free, since huge areas are colored in red, yellow and green. But drawing a bus is more regular with more concentrated focuses.

The deviation of variant levels among categories inspires us to further explore the connection between the approaches for using drawing orders and their sketch representing performance. We select SketchHealer 2.0, SP-gra2seq and DC-gra2seq for comparison, since they make (no) use of drawing orders by different approaches. We compute their controllable

Table 4: Controllable sketch synthesis (Mask = 0%) and sketch healing (Mask = 10%, 30%) performances of DC-gra2seq by allowing PEs to participate in the construction of graph nodes, edges or not. “Node ✓ Edge ×” denotes the proposed DC-gra2seq.

Mask	Node	Edge	DS1			DS2			DS3					
			<i>Rec</i>	<i>Ret</i>		<i>Rec</i>	<i>Ret</i>		<i>Rec</i>	<i>Ret</i>				
				@1	@10	@50		@1	@10	@50		@1	@10	@50
0%	×	×	94.51	80.90	95.09	98.19	85.84	41.00	71.80	87.31	83.93	57.50	83.52	93.45
	✓	×	96.26	96.84	99.48	99.88	95.70	92.75	98.08	99.42	90.41	96.27	99.47	99.81
	×	✓	95.69	79.22	93.92	97.77	92.41	67.49	88.30	95.30	88.48	76.25	92.64	97.24
	✓	✓	95.91	95.66	99.23	99.78	94.67	90.00	97.88	99.32	89.05	94.74	99.44	99.75
10%	×	×	92.55	40.69	65.64	79.69	90.08	41.08	66.21	80.72	83.84	39.03	62.23	76.74
	✓	×	94.45	74.59	88.83	94.31	92.64	67.61	84.31	91.17	85.21	71.66	86.34	92.35
	×	✓	93.48	50.64	75.10	87.46	89.48	45.24	70.13	83.33	84.79	46.77	70.37	82.90
	✓	✓	93.96	70.56	86.10	92.56	91.55	67.10	84.08	91.02	85.18	69.96	86.67	92.43
30%	×	×	82.18	10.93	26.52	42.02	77.20	10.80	25.61	45.56	70.35	4.72	15.05	29.47
	✓	×	86.50	30.30	51.38	65.84	84.62	29.92	49.26	62.44	72.84	27.64	47.34	60.61
	×	✓	84.23	16.28	36.80	55.01	80.40	18.62	37.78	53.70	71.99	14.56	31.54	47.96
	✓	✓	85.00	26.15	45.94	61.06	83.94	29.38	48.55	62.22	72.26	25.88	46.33	59.82

synthesis performances on every single category in DS1, shown in Table 3. By checking the values in each column, we find that buses contribute the most while pigs contribute the least to the performance on the full DS1, which is consistent with the observation in Fig. 4. It supports the assumption that variations of sketch drawings could reduce the representing performance as expected. Furthermore, our DC-gra2seq yields the smallest gap on performance between pig and bus, while SketchHealer 2.0 gets the largest. It could be an evidence to support our DC-gra2seq is protected from variants of sketch drawings by injecting drawing orders into graph nodes.

4.5. The impact of injecting drawing orders into nodes or edges

We further discuss the impact of injecting sketch drawing orders into graph nodes, edges or both via PEs. To make PEs access to edge construction, we adopt the computation of self-attention scores in vanilla self-attention network [10], i.e., $\alpha^{\text{atten}}(i, j) = (\mathbf{v}_{ii} + \mathbf{P}(i))^\top (\mathbf{v}_{jj} + \mathbf{P}(j))$. A softmax activation function is applied over A_t in Eq. (6) before sent into Eq. (8) for message aggregation.

Table 4 presents the experimental results on three datasets. When PEs attend the edge construction only (Node ×, Edge ✓), it outperforms the version which never uses PEs (Node ×, Edge ×) in most cases. The usage of drawing orders via PEs embedded graph edges is beneficial to improve sketch learning, but the performance gain is sensitive to various sketch drawings, e.g., it significantly outperforms “Node ×, Edge ×” on *Rec* in DS2, but is defeated on top-1, top-10 *Ret* in DS1. Similarly, our DC-gra2seq (Node ✓, Edge ×) outperforms “Node ✓, Edge ✓” in most cases. As a result, embedding drawing orders into graph nodes is a proper way to make better use of sequential information.

5. Conclusions

We have presented DC-gra2seq to encode sketch drawing orders by PE for learning context-aware graphic sketch represen-

tations. Each sketch patch is equipped with a sinusoidal absolute PE, indicating where it is drawn in a drawing order, and a learnable relative PE, restoring the sequential information from the contextual positions of sketch components. The attendance of PEs encourages DC-gra2seq to simultaneously consider both the visual patterns from the canvas and the sequential positions from the drawing order, which benefits sketch representation learning verified on controllable sketch synthesis and sketch healing.

6. Acknowledgments

This work was supported by the Joint Funds of the National Natural Science Foundation of China (U2033218).

References

- [1] G. Su, Y. Qi, K. Pang, J. Yang, Y.-Z. Song, Sketchhealer: a graph-to-sequence network for recreating partial human sketches, in: Proceedings of The 31st British Machine Vision Virtual Conference, British Machine Vision Association, 2020, pp. 1–14.
- [2] Y. Qi, G. Su, Q. Wang, J. Yang, K. Pang, Y.-Z. Song, Generative sketch healing, International Journal of Computer Vision (2022) 1–16.
- [3] J. Song, K. Pang, Y.-Z. Song, T. Xiang, T. M. Hospedales, Learning to sketch with shortcut cycle consistency, in: Proceedings of the IEEE Conference on Computer Vision and Pattern Recognition, 2018, pp. 801–810.
- [4] P. Xu, Y. Huang, T. Yuan, K. Pang, Y.-Z. Song, T. Xiang, T. M. Hospedales, Z. Ma, J. Guo, Sketchmate: Deep hashing for million-scale human sketch retrieval, in: Proceedings of the IEEE Conference on Computer Vision and Pattern Recognition, 2018, pp. 8090–8098.
- [5] P. Xu, Y. Huang, T. Yuan, T. Xiang, T. M. Hospedales, Y.-Z. Song, L. Wang, On learning semantic representations for large-scale abstract sketches, IEEE Transactions on Circuits and Systems for Video Technology 31 (9) (2020) 3366–3379.
- [6] P. Xu, Z. Song, Q. Yin, Y.-Z. Song, L. Wang, Deep self-supervised representation learning for free-hand sketch, IEEE Transactions on Circuits and Systems for Video Technology 31 (4) (2020) 1503–1513.
- [7] T. N. Kipf, M. Welling, Semi-supervised classification with graph convolutional networks, arXiv preprint arXiv:1609.02907 (2016).
- [8] S. Zang, S. Tu, L. Xu, Linking sketch patches by learning synonymous proximity for graphic sketch representation, in: Proceedings of the AAAI Conference on Artificial Intelligence, Vol. 37, 2023, pp. 11096–11103. doi:<https://doi.org/10.1609/aaai.v37i9.26314>.

- [9] J. Gehring, M. Auli, D. Grangier, D. Yarats, Y. N. Dauphin, Convolutional sequence to sequence learning, in: *International Conference on Machine Learning*, PMLR, 2017, pp. 1243–1252.
- [10] A. Vaswani, N. Shazeer, N. Parmar, J. Uszkoreit, L. Jones, A. N. Gomez, Ł. Kaiser, I. Polosukhin, Attention is all you need, *Advances in Neural Information Processing Systems* 30 (2017).
- [11] Y. Chen, S. Tu, Y. Yi, L. Xu, Sketch-pix2seq: a model to generate sketches of multiple categories, arXiv preprint arXiv:1709.04121 (2017).
- [12] S. Zang, S. Tu, L. Xu, Controllable stroke-based sketch synthesis from a self-organized latent space, *Neural Networks* 137 (2021) 138–150.
- [13] S. Zang, S. Tu, L. Xu, Self-organizing a latent hierarchy of sketch patterns for controllable sketch synthesis, *IEEE Transactions on Neural Networks and Learning Systems* (2023).
- [14] T. Li, S. Zang, S. Tu, L. Xu, Lmsr-pix2seq: Learning stable sketch representations for sketch healing, *Computer Vision and Image Understanding* 240 (2024) 103931.
- [15] D. Ha, D. Eck, A neural representation of sketch drawings, in: *International Conference on Learning Representations*, 2018.
- [16] K. Li, K. Pang, J. Song, Y.-Z. Song, T. Xiang, T. M. Hospedales, H. Zhang, Universal sketch perceptual grouping, in: *Proceedings of the European Conference on Computer Vision*, 2018, pp. 582–597.
- [17] L. S. F. Ribeiro, T. Bui, J. Collomosse, M. Ponti, Sketchformer: Transformer-based representation for sketched structure, in: *Proceedings of the IEEE/CVF Conference on Computer Vision and Pattern Recognition*, 2020, pp. 14153–14162.
- [18] H. Lin, Y. Fu, X. Xue, Y.-G. Jiang, Sketch-bert: Learning sketch bidirectional encoder representation from transformers by self-supervised learning of sketch gestalt, in: *Proceedings of the IEEE/CVF Conference on Computer Vision and Pattern Recognition*, 2020, pp. 6758–6767.
- [19] Y. Qi, G. Su, P. N. Chowdhury, M. Li, Y.-Z. Song, Sketchlattice: Latticed representation for sketch manipulation, in: *Proceedings of the IEEE/CVF International Conference on Computer Vision*, 2021, pp. 953–961.
- [20] H. Li, X. Jiang, B. Guarn, N. M. Thalmann, Efficient sketch recognition via compact spatial embedding graph neural networks, in: *2021 IEEE International Conference on Multimedia and Expo*, IEEE, 2021, pp. 1–6.
- [21] P. Xu, C. K. Joshi, X. Bresson, Multigraph transformer for free-hand sketch recognition, *IEEE Transactions on Neural Networks and Learning Systems* 33 (10) (2021) 5150–5161.
- [22] L. Yang, A. Sain, L. Li, Y. Qi, H. Zhang, Y.-Z. Song, S3net: Graph representational network for sketch recognition, in: *2020 IEEE International Conference on Multimedia and Expo*, IEEE, 2020, pp. 1–6.
- [23] A. Qi, Y. Gryaditskaya, T. Xiang, Y.-Z. Song, One sketch for all: One-shot personalized sketch segmentation, *IEEE Transactions on Image Processing* 31 (2022) 2673–2682.
- [24] L. Yang, J. Zhuang, H. Fu, X. Wei, K. Zhou, Y. Zheng, Sketchgnn: Semantic sketch segmentation with graph neural networks, *ACM Transactions on Graphics* 40 (3) (2021) 1–13.
- [25] Z. Zhang, Y. Zhang, R. Feng, T. Zhang, W. Fan, Zero-shot sketch-based image retrieval via graph convolution network, in: *Proceedings of the AAAI Conference on Artificial Intelligence*, Vol. 34, 2020, pp. 12943–12950.
- [26] F. Scarselli, M. Gori, A. C. Tsoi, M. Hagenbuchner, G. Monfardini, The graph neural network model, *IEEE Transactions on Neural Networks* 20 (1) (2008) 61–80.
- [27] P. Veličković, G. Cucurull, A. Casanova, A. Romero, P. Lio, Y. Bengio, Graph attention networks, arXiv preprint arXiv:1710.10903 (2017).
- [28] P. Shaw, J. Uszkoreit, A. Vaswani, Self-attention with relative position representations, arXiv preprint arXiv:1803.02155 (2018).
- [29] Z. Dai, Z. Yang, Y. Yang, J. Carbonell, Q. V. Le, R. Salakhutdinov, Transformer-xl: Attentive language models beyond a fixed-length context, arXiv preprint arXiv:1901.02860 (2019).
- [30] K. Wu, H. Peng, M. Chen, J. Fu, H. Chao, Rethinking and improving relative position encoding for vision transformer, in: *Proceedings of the IEEE/CVF International Conference on Computer Vision*, 2021, pp. 10033–10041.
- [31] X. Wang, Z. Tu, L. Wang, S. Shi, Self-attention with structural position representations, arXiv preprint arXiv:1909.00383 (2019).
- [32] X. Chu, Z. Tian, B. Zhang, X. Wang, C. Shen, Conditional positional encodings for vision transformers, in: *The Eleventh International Conference on Learning Representations*, 2022.
- [33] J. Su, M. Ahmed, Y. Lu, S. Pan, W. Bo, Y. Liu, Roformer: Enhanced transformer with rotary position embedding, *Neurocomputing* 568 (2024) 127063.
- [34] D. P. Kingma, M. Welling, Auto-encoding variational bayes, in: *International Conference on Learning Representations*, 2014.
- [35] Q. Yu, Y. Yang, Y.-Z. Song, T. Xiang, T. Hospedales, Sketch-a-net that beats humans, in: *British Machine Vision Conference*, 2015.